Heat Transfer—Asian Research, **34** (8), 2005

Mixed Convective Heat Transfer of Water in a Pipe under Supercritical Pressure

Feng Xu, Liejin Guo, and Bofeng Bai
State Key Laboratory of Multiphase Flow in Power Engineering,
Xi'an Jiaotong University, Xi'an, China

Because of the rapid properties variation of fluid under supercritical pressure, there is a violent secondary flow in a heated pipe, which will certainly complicate the heat transfer of fluid in a pipe under supercritical pressure. In this paper, a numerical study is conducted for the laminar developing mixed convective heat transfer of water under supercritical pressure. The velocity field and temperature field are given, and the influence of different parameters on flow and heat transfer is investigated in detail. The results show that secondary flow has a great influence on velocity and temperature distributions and thus affects the friction factor and the Nusselt number remarkably.
 Heat Trans Asian Res, 34(8): 608–619, 2005; Published online in Wiley InterScience (www.interscience.wiley.com). DOI 10.1002/htj.20079

Key words: supercritical, pseudo-critical, mixed convection, secondary flow, heat transfer

1. Introduction

Because of a wide range of applications, forced convection of fluids under supercritical pressure, such as water, carbon dioxide, nitrogen, hydrogen, and helium, in channels has been extensively studied both experimentally and numerically. Kurganov measured the turbulent velocity and temperature distribution of CO_2 flowing in a vertical heated tube under supercritical pressure [1]. In the experiment, a protruding shaped velocity profile was obtained in a downward flow and an "M" shaped velocity profile was observed in an upward flow. In Wood's experiment of supercritical CO_2 [2], a similar "M" shaped velocity profile was obtained in the upward flow, and the maximum velocity appeared at a location deviating from the tube axis.

Morton first pointed out that buoyancy forces may cause two symmetrical vortices perpendicular to the main flow [3], which is referred to as Morton vortices. Thus under supercritical pressure, the sharp variation of fluid properties will certainly result in a very large secondary flow in a horizontal heated pipe, which will no doubt have a great influence on the flow and heat transfer characteristics. For the flow in the straight pipe, all of the experimental studies of Domin [4], Schmidt [5], Vikrev

Contract grant sponsor: National Key Basic Research Projects under contract No. 2003CB214500 and No. G1999022308.

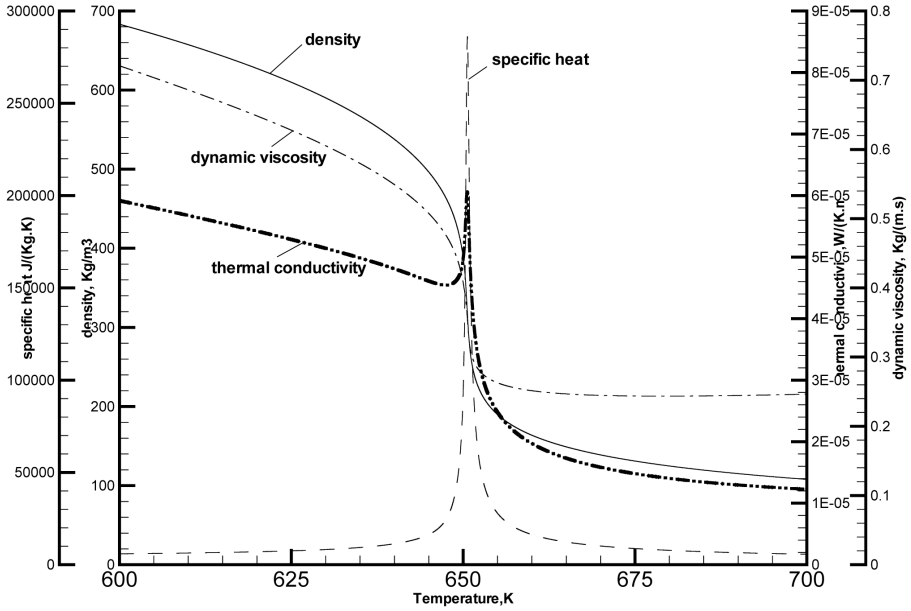

Fig. 1. Variation of water properties at pressure P = 23 MPa.

and Lokshin [6], and Griffith and Sciralkar [7] showed that an abrupt increase of wall temperature occurred on a very large area of the heat transfer surface, which means that heat transfer deterioration in straight flow is not a local phenomenon.

One of the most important characteristics of supercritical fluids near the critical point is that their physical properties exhibit sharp variations with the change of temperature and pressure, especially near the pseudo-critical point (the temperature at which the specific heat reaches a peak for a given pressure). The variation of specific heat, density, thermal conductivity, and dynamic viscosity of water with temperature at pressure 23 MPa is shown in Fig. 1. These physical property curves are plotted based on the IAPWS Formulation 1995 [8].

Most of the previous investigations have been concerned with turbulent flows in tubes. It is well known that gravity has a strong effect on the flow pattern and heat transfer characteristics under supercritical pressure. In order to better understand the gravity effect, in this paper, a numerical study was carried out for the laminar flow of water under supercritical pressure in both vertical and horizontal smooth pipes. The analysis sheds light on the interactions between the secondary flow and the developing temperature field for supercritical pressure fluids.

Nomenclature

D: tube diameter, m

e: enthapy, kJ kg^{-1}

f: skin friction coefficient defined by Eq. (11)

g: gravity, $m \cdot s^{-2}$
Gr: Grashof number defined by Eq. (14)
L: tube length, m
Nu: Nusselt number
P: pressure, MPa
Pr: Prandtl number
Re: Reynolds number
R: tube radius, m
T: temperature, K
u: velocity, $m \cdot s^{-1}$
ρ: density, $kg \cdot m^{-3}$

Subscripts and Superscripts

ax: axial direction
b: bulk flow
c: critical
in: inlet
pc: pseudo-critical
w: wall

2. Numerical Model and Numerical Method

2.1 Formulation

We consider a steady, laminar flow in a vertical tube (with diameter D = 0.01 m and length L, L/D = 15) and a horizontal tube (with diameter D = 0.01 m and length L, L/D = 20) heated at a constant heat flux q_w in the presence of gravity. The governing conservative equations are given by

Mass:

$$\partial\rho/\partial t + \nabla \cdot \rho u = 0 \tag{1}$$

Momentum:

$$\partial\rho u/\partial t + \nabla \cdot \rho uu = -\nabla \cdot p + \nabla \cdot \tau - g \tag{2}$$

Energy:

$$\partial\rho e/\partial t + \nabla \cdot \rho uh = -\nabla \cdot \lambda\nabla T + dp/dt + \tau : \nabla u \tag{3}$$

where $\tau = \eta(\nabla u + \nabla u^T) - 2/3\eta(\nabla \cdot u)$, p represents the pressure of the fluid.

The boundary conditions are

at the wall:

$$u = 0,\ v = 0,\ q = q_{\mathrm{w}} \tag{4}$$

at the inlet:

$$e = e(T_{\mathrm{in}}),\ u = u_{\mathrm{in}},\ v = 0 \tag{5}$$

at the outlet:

$$(\partial e/\partial x)_{x=L} = 0,\ (\partial u/\partial x)_{x=L} = 0 \tag{6}$$

at the centerline:

$$(\partial u/\partial r)_{r=0} = 0,\ (\partial e/\partial r)_{r=0} = 0 \tag{7}$$

2.2 Numerical method

A numerical solution to Eqs. (1) to (7) was solved by a CFD solver, FLUENT 6.0, which used a control-volume finite element method (CVFEM). The coupling between pressure and velocity is handled by a SIMPLEC algorithm. Due to the large variation of the properties, the under-relaxation technique was adopted in the iteration procedure, with under-relaxation factors ranging from 0.1 to 0.3 for all independent variables and thermodynamic properties. Grid independence of the solution was checked by refining the radial and axial grid system. The convergent solution is obtained when the following convergence criteria are satisfied for all independent variables:

$$\left| \frac{\Phi^{i+1} - \Phi^{i}}{\Phi^{i}} \right| \le 10^{-3},\ \Phi = u,\ v, \text{ and } e \tag{8}$$

3. Numerical Results and Analysis

In this paper, the dimensionless temperature and velocity are used, which are defined as follows:

$$u^{*} = u/u_{\mathrm{in}}, \tag{9}$$

$$\theta = (T - T_{\mathrm{in}})/(T_{\mathrm{w}} - T_{\mathrm{in}}) \tag{10}$$

Friction coefficient is based on the section average fluid properties, defined as follows:

$$f = 4\tau_{W}/\overline{(0.5\rho \cdot u^{2})} \tag{11}$$

where

$$\overline{(0.5\rho \cdot u^2)} = \frac{1}{A}\int_A 0.5\rho u^2 dA \tag{12}$$

Through setting up the balance between work done by specific buoyancy forces and the resulting specific kinetic energy of the secondary flow, and taking the influence of the *Pr* number into account, we get the relative magnitude of the secondary flow due to buoyancy forces [9]:

$$\tilde{u}_{Gr}/\tilde{u}_{\mathrm{ax}} = \theta(\sqrt{Gr}/(Re\sqrt{(1+Pr)})) \tag{13}$$

The Grashof number is defined as:

$$Gr = g\beta\rho^2 d^4 q''/\mu^2 k \text{ or } g\beta\rho^2 d^3 \Delta T/\mu^2 \tag{14}$$

The magnitude of the secondary flow is expressed as a ratio of the kinetic energy of the secondary flow to the kinetic energy of the primary flow and is defined as

$$K = \int_A u_{\mathrm{sec}}^2 dydz / \int_A u_{\mathrm{ax}}^2 dydz \tag{15}$$

where $u_{\mathrm{sec}} = \sqrt{v^2 + w^2}$ and u_{ax} is the axial velocity.

3.1 Data comparison

In order to verify the accuracy of the computational model, the developing laminar heat transfer in a horizontal heated pipe of $L/D = 40$ is computed under $P = 23$ MPa and constant wall temperature boundary conditions, and the results are compared with those calculated from the empirical correlations of Colburn [10] and Oliver [11], as shown in Fig. 2. From the figure we can see that, there exists a good agreement between numerical prediction and that of Oliver [11]. But there is a large deviation from Colburn [10]. This is because in the empirical correlation of Colburn, the fluid film temperature T_{f} is used, which has no definite definition.

3.2 Mixed convective heat transfer in vertical pipe

3.2.1 Velocity profiles and temperature profiles

Figure 3(a) shows the dimensionless velocity profiles and Fig. 3(b) shows the dimensionless temperature profiles at different locations along the tube under the conditions of constant heat flux ($q_w = 50$ W/m^2), $p = 23$ MPa, $T_{\mathrm{in}} = 647$ K, $Re_{\mathrm{in}} = 1000$, and $Gr = 2.87 \times 10^7$. From the velocity profiles, it can be seen that the buoyancy effect due to density variation near the wall is large compared with the shear stress induced by deceleration of the fluid. The velocity of the fluid near the wall increases along the tube from the inlet and there appears a velocity peak near the wall, which increases continuously along the pipe until buoyancy effects become negligible. It can also be seen that velocity at the centerline decreases continuously, which means that recirculation or reverse flow may appear in the downstream core region of the tube. Since the fluid temperature is close to a pseudo-critical

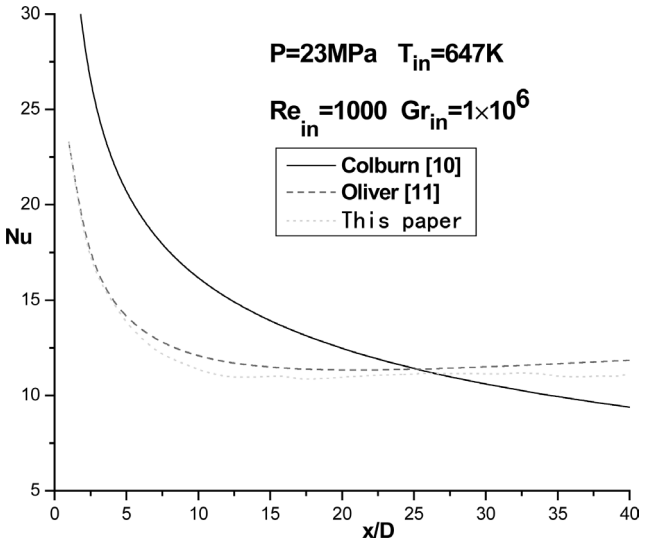

Fig. 2. Comparison with other studies.

value (T_{pc} = 650.65 K at 23 MPa), properties vary violently with temperature. Under the effect of gravity, the fluid with a smaller density is accelerated upward. The velocity decrease rate at the centerline depends on many parameters. For the near critical region, the inlet conditions are important because the variation of properties is different for each pressure and temperature. The radial velocity component has a direction toward the wall over much of the tube radius in order to satisfy mass conservation, which means that streamlines move toward the wall along the tube. From the temperature profiles, we can see that there is a variation of temperature only in a very narrow near wall region ($r/R > 0.65$), which results in large variations of fluid properties, and then undoubtedly influences

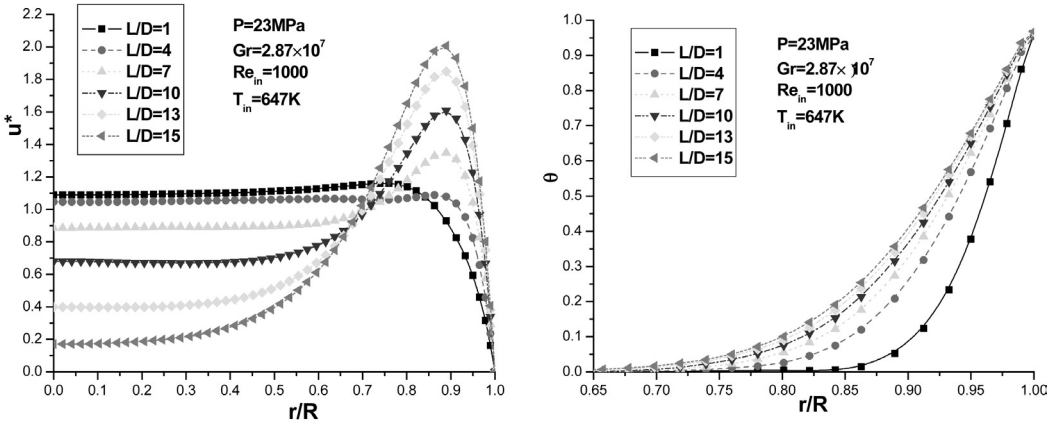

(a) Velocity distribution

(b) Temperature distribution

Fig. 3. Dimensionless velocity and temperature profiles along the pipe.

local heat transfer characteristics. But it should be noted that the temperature distribution is not so severely deformed as might be expected with these properties' variations.

3.2.2 Influence of flow orientation on flow friction and heat transfer

Figure 4 shows the variation of the product of friction factor and Reynolds number and the variation of Nusselt number along the tube under the conditions of constant heat flux ($q_w = 50$ W/m^2), $p = 23$ MPa, $T_{in} = 647$ K and $Re_{in} = 1000$. At the same time the ratio of Nu and ratio of $f \cdot Re$ between that with a gravity effect and that without a gravity effect are also given. With the inclusion of the gravity effect, the friction of upward flow is much larger than that of downward flow, and both are larger than those without the gravity effect. The heat transfer coefficient including the gravitational body force has a relatively large value compared with that neglecting the gravity force. This difference is caused by the high convection of the buoyancy-induced rapidly accelerating fluid near the wall. At the place where the difference is largest, Nu and $f \cdot Re$ with gravity effect are respectively 2.2 and 8.3 times those without gravity effect. The result with a Boussinesq assumption is smaller than that with variable properties, and the largest error is about 10%. This is due to the limitation of Boussinesq assumption in which only density variation is considered and the variation of density with temperature is taken as linear. But under supercritical pressure, all properties vary violently with temperature non-linearly, so Boussinesq assumption cannot be used here.

3.3 Mixed convective heat transfer in horizontal pipe

3.3.1 Velocity and temperature profiles

Figure 5 gives the velocity and temperature fields at the locations of $x/D = 5$, 10, and 20 under the conditions of $P = 23$ MPa, $Re_{in} = 1000$ and $T_{in} = 647$ K and different inlet Grashof numbers (the relative magnitude of buoyancy caused secondary flow to bulk flow for $Gr = 1 \times 10^6$, 1×10^7 is 0.795 and 2.51 respectively). The left side of the pictures shows contours of axial velocity and vectors of the secondary velocity components. The right side of the pictures shows temperature contours with

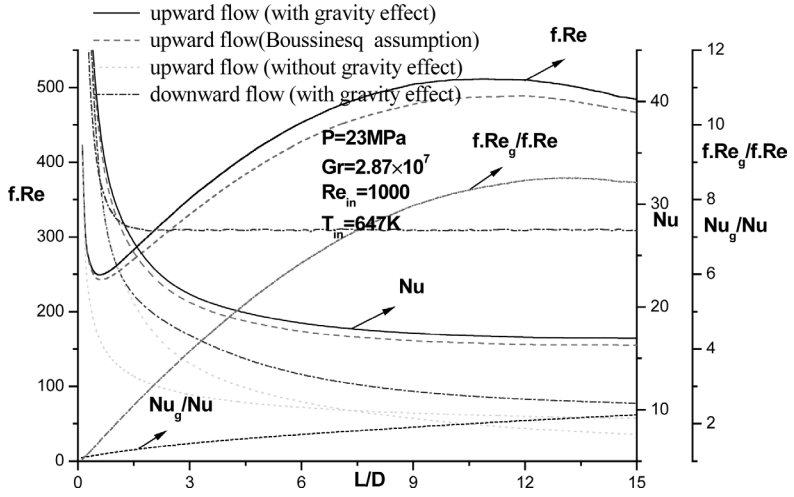

Fig. 4. Influence of flow orientation on friction and heat transfer.

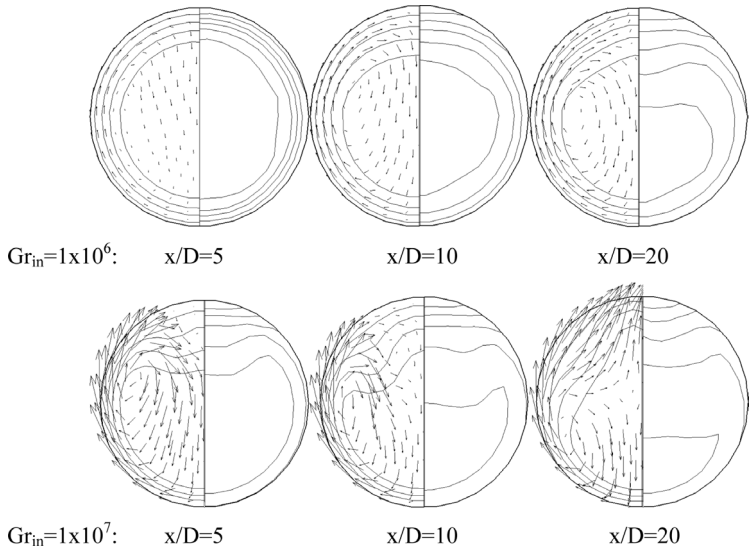

Fig. 5. Velocity and temperature fields at the locations of *x/D* = 5, 10, and 20. (Left side is the velocity profile and the right side is the temperature profile.)

a difference in value of 0.2 ΔT (temperature difference between wall temperature and bulk temperature). In a heated horizontal pipe, the fluid is heated at the wall, thus the fluid in the near wall region will have a lower density than that in the core of the pipe. The corresponding temperature gradient results in a buoyancy force, which results in the upward flow of the fluid in the near wall region, and the fluid will certainly flow downward from the core due to mass conservation. Thus the Morton type secondary flow is formed as shown in Fig. 5.

Comparing the vectors of the secondary flow pattern for different Grashof numbers, we can clearly see that the secondary flow is relatively intensified with the increase of Grashof number. The secondary velocity near the wall is obviously larger than that in the core region. At $Gr = 1 \times 10^6$, secondary flow gets larger continuously along the pipe; but at $Gr = 1 \times 10^7$, the secondary flow at the location of *x/D* = 5 is clearly larger than those at the locations of *x/D* = 10 and 20, which can also be seen in Fig. 5. The secondary flow consists of one vortex on either side of the pipe, and the center of this vortex is observed to shift downward along the pipe (at location of *x/D* = 20, it is almost shifted to $z = 0$). It is more obvious for higher Grashof numbers.

From the temperature field we can also see the influence of secondary flow. In the same axial section, due to the downward flow of fluid in the core, the bulk fluid is shifted downward, thus the thermal boundary layer at the lower side is small. At the same time, the heated fluid flows upward at the wall, along which the thermal boundary layer grows.

3.3.2 Influence of the inlet Reynolds number

Figure 6 gives the development of secondary flow, friction, and heat transfer along the pipe for different inlet Reynolds numbers under the conditions of $P = 23$ MPa, $T_{in} = 647$ K, and $Gr_{in} = 1 \times 10^6$. With the increase of Reynolds numbers, the corresponding relative magnitude of secondary

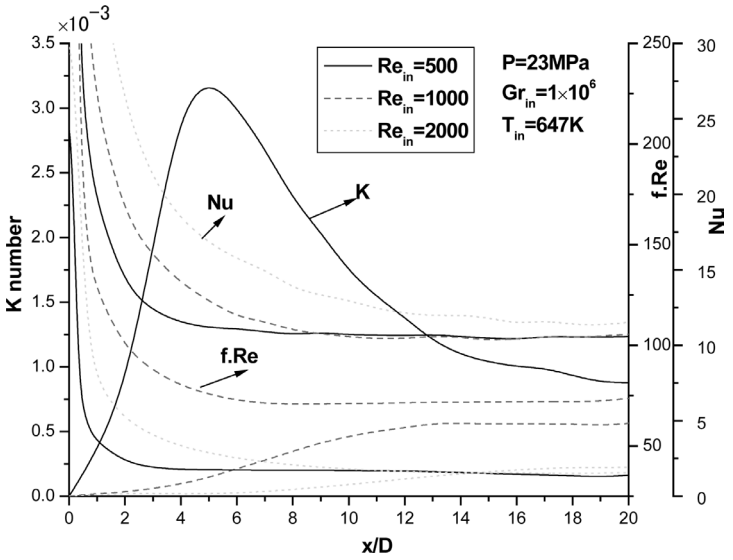

Fig. 6. Influence of inlet Reynolds number.

flow is 1.59, 0.795, and 0.398, respectively. From the figure we can see that for all situations, the relative kinetic energy K initially increases up to a maximum value and then decreases. This is because in the first part of the pipe, due to the effect of buoyancy the secondary flow gains momentum; but along the pipe, because of the heat balance between the fluid and wall, the buoyancy forces decrease gradually, resulting in the decrease of K. In general, the higher the Gr, the stronger the secondary flow and the sooner the maximum in K has been reached. Yousef and Tarasuk [13] in their experiment also found that there appeared a maximum value of the secondary flow near the entrance of the pipe. It can also be seen that, the smaller the inlet Reynolds number, the larger the relative magnitude of the secondary flow, and thus the larger value of K. What deserves attention is that it is for $Re_{\text{in}} = 1000$ that the product $f \cdot Re$ has the largest value. According to boundary layer theory, the velocity boundary layer increases with decreasing Reynolds number, which means that the velocity gradient and thus the friction decrease with a decreasing Reynolds number. On the other hand, the secondary flow intensity and the corresponding friction caused by the secondary flow increase with a decreasing Reynolds number. Therefore, there should exist a mediate value of Reynolds number where the product $f \cdot Re$ reaches the maximum. It can also be seen that there is intersection of curves for $Re_{\text{in}} = 2000$ and for $Re_{\text{in}} = 500$, which is because the relative magnitude of secondary flow for $Re_{\text{in}} = 500$ is larger than for $Re_{\text{in}} = 2000$. The Nusselt number increases with the increase of the Reynolds number. This is because that at a specific Prandtl number, the thermal boundary layer decreases with an increasing Reynolds number according to boundary layer theory. But because of the effect of secondary flow, the Nusselt number for $Re_{\text{in}} = 500$ exceeds that for $Re_{\text{in}} = 1000$ at the location of $x/D = 8$.

3.3.3 Influence of inlet fluid temperature

Figure 7 gives the influence of inlet fluid temperature on the kinetic energy of the secondary flow K, friction $f \cdot Re$ and the Nusselt number along the pipe under the conditions of $P = 23$ MPa, $Re_{\text{in}} = 1000$, and $Gr_{\text{in}} = 1 \cdot 10^6$. It shows that the kinetic energy of the secondary flow K decreases as the

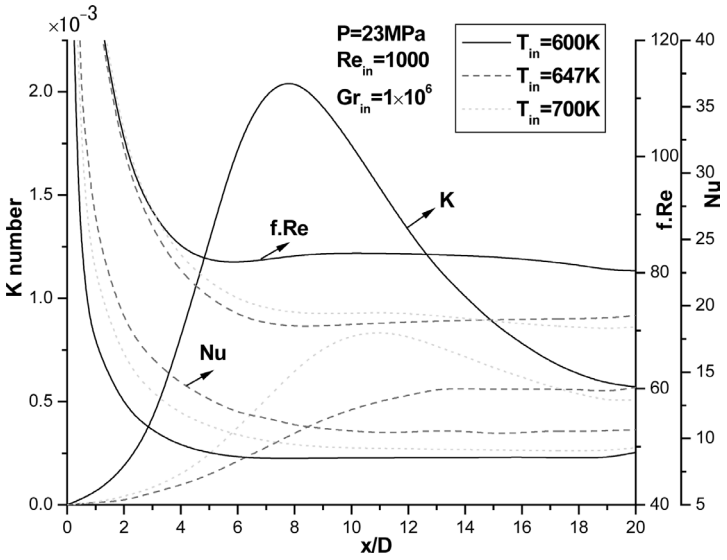

Fig. 7. Influence of inlet fluid temperature.

inlet fluid temperature approaches the pseudo-critical temperature due to the increases of Prandtl numbers (for 23 MPa, the corresponding Pr for T_{in} = 600 K, 647 K, and 700 K is 0.912, 2.954, and 1.452, respectively), thus the corresponding relative magnitude of secondary flow to bulk flow is 1.143, 0.795, and 1.01. The decrease of secondary flow intensity means that the fluid near the wall decreases and the corresponding velocity boundary layer increases, resulting in the decrease of friction. Therefore, with the inlet fluid temperature approaching the pseudo-critical value, the product $f \cdot Re$ decreases. It can be seen that in the case of T_{in} = 600 K, there appears a peak of $f \cdot Re$ at the location of $x/D \approx 9$ where the secondary flow intensity reaches its maximum value. The Nusselt number gets larger with the inlet fluid temperature approaching the pseudo-critical value. For developing forced convective flow, it can be deduced using boundary layer analysis that the thermal boundary layer approximately scales with $Pr^{-1/3}$ for larger Prandtl numbers [12]. Thus the thermal boundary layer thickness is approximately 1:0.697:0.883; in the forced convective case, and the scale of Nusselt numbers is approximately 1:1.435:1.132. In spite of the decrease of secondary flow with the inlet fluid temperature approaching the pseudo-critical value, the difference of thermal boundary layer for different inlet fluid temperatures is so large that the influence of secondary flow is not obvious. But from the figure we can see that the larger of the secondary flow, the closer the minimum value of the Nusselt number to the entrance.

4. Conclusions

In order to better understand the influence of gravity on the flow and heat transfer of supercritical fluids, a numerical study has been conducted for the developing laminar flow and heat transfer of water in smooth vertical and horizontal tubes under supercritical pressure. Although a small heat flux is applied and induces very small temperature gradients, the variation of properties, especially density as reflected in the gravity effect, cannot be neglected near the critical region. The buoyancy effect strongly influences the flow pattern and heat transfer characteristics in the critical region. The main conclusions are

1) Due to the effect of buoyancy, the velocity profile of supercritical water in pipe flow is deformed from that with constant properties or without gravity effect, which is not a parabola any more, but in the shape of "M." There appears a velocity peak near the wall, instead of centerline. With the inlet fluid temperature approaching the pseudo-critical temperature, buoyancy effects on the forced convection increase rapidly, resulting in an increased fluid velocity near the heated wall, and a decreased thermal boundary layer thickness.

2) Gravity affects both the friction factor and Nusselt number. In the presence of gravity, the friction factor of the developing laminar flow of the supercritical fluid is much larger than that of the fully developed laminar flow with constant properties; and the friction factor of the upward flow is larger than that of the downward flow. Both the friction factor and Nusselt number with gravity effect are greater than those without gravity effect; and compared with variable property results, both the friction factor and Nusselt number obtained with Boussinesq assumption are a little smaller.

3) Under supercritical pressure, due to the sharp variation of fluid property, there appears a very large secondary flow in the vertical direction of a horizontal heated pipe, making the bulk flow shift downward, and thus it has a great influence on the friction and heat transfer. The relative kinetic energy K initially increases up to a maximum value and then decreases. The larger the secondary flow, the closer of the extremum of K, $f \cdot Re$, and Nu to the entrance of the pipe.

4) The relative kinetic energy K increases with the decrease of the inlet Reynolds number; the secondary flow grows with a decreasing Reynolds number, but the velocity gradient near the wall is so small that it exceeds the influence of secondary flow. With the inlet fluid temperature approaching the pseudo-critical value, the Prandtl number increases, K deceases, and $f \cdot Re$ also decreases correspondingly; but the difference of thermal boundary layer for different inlet fluid temperature is so large that the influence of secondary flow is not obvious. The Nusselt number gets larger with the inlet fluid temperature approaching the pseudo-critical value.

Acknowledgments

This work is supported by the National Key Basic Research Projects with contract No. 2003CB214500 and No. G1999022308.

Literature Cited

1. Kurganov VA, Kaptilnyi AG. Flow structure and turbulent transport of a supercritical pressure fluid in a vertical heated tube under the conditions of mixed convection. Experimental Data Int J Heat Mass Transfer 1993;36:3383–3392.
2. Wood RD, Smith JM. Heat transfer in the critical region-temperature and velocity profiles in turbulent flow. AIChE J 1964;10:180–186.
3. Morton BR. Laminar convection in uniform heated horizontal pipes at low Rayleigh numbers. Q J Masliyah 1959;12:410–420.
4. Domin G. Warmeubergang in kritischen und uberkritischen Bereichen von Wasser in Rohren BWK 1963;15(11).
5. Schmidt KR. Thermal investigations with heavily loaded boiler heating surface. Mitt Ver Grosselbetr 1959;63.

6. Vikrev YV, Lokshin VA. An experimental study of temperature conditions in horizontal steam generating tubes at supercritical pressures. Teploenergetika 1964;11, 12.
7. Griffith P, Sciralkar BS. The deterioration in heat transfer to fluids at supercritical pressure and high heat flux. Dept Mech Eng, MIT Rept, 1968, 70332–70351.
8. Wagner W, Pruß A. The IAPWS formulation 1995 for the thermodynamic properties of ordinary water substance for general and scientific use. J Phys Chem Ref Data 2002;31(2).
9. Sillekens JM. Laminar mixed convection in ducts. 1995.
10. Colburn AP. A method for correlating forced convective heat transfer data and comparison with fluid friction. Trans AIChe 1933;29:174–210.
11. Oliver DR. The effect of natural convection on viscous flow heat transfer in horizontal tubes. Chem Eng Sci 1962;17:335–350.
12. Schlichting H. Boudary-Layer theory. 7th ed. McGraw-Hill Book Co.; 1979.
13. Yousef WW, Tarasuk JD. An interferometric study of combined free and forced convection in a horizontal isothermal tube. J Heat Transfer 1981;103:249–256.

□♦ ♦ ♦□

Originally published in *Journal of Engineering Thermophysics* **26**(1), 2005, 76–79.
Translated by Feng Xu, State Key Laboratory of Multiphase Flow in Power Engineering, Xi'an Jiaotong University, Xi'an 710049, China.